Universiteit
Leiden
The Netherlands

The role of the Arabidopsis AHL15/REJUVENATOR gene in developmental phase transitions

Karami, O.; Karami O.

Citation
Karami, O. (2017, September 5). *The role of the Arabidopsis AHL15/REJUVENATOR gene in developmental phase transitions*. Retrieved from https://hdl.handle.net/1887/54683

Version:	Not Applicable (or Unknown)
License:	Licence agreement concerning inclusion of doctoral thesis in the Institutional Repository of the University of Leiden
Downloaded from:	https://hdl.handle.net/1887/54683

Note: To cite this publication please use the final published version (if applicable).

Cover Page

Universiteit Leiden

The handle http://hdl.handle.net/1887/54683 holds various files of this Leiden University dissertation

Author: Karami, Omid
Title: The role of the Arabidopsis AHL15/REJUVENATOR gene in developmental phase transitions
Issue Date: 2017-09-05

Chapter 2

An Arabidopsis AT-hook motif nuclear protein mediates somatic-to-embryonic cell fate conversion coinciding with genome duplication

Omid Karami[1], Arezoo Rahimi[1], Patrick Mak[2,3], Anneke Horstman[4], Kim Boutilier[4], Monique Compier[2,5], Bert van der Zaal[1] and Remko Offringa[1]

[1]Plant Developmental Genetics, Institute of Biology Leiden, Leiden University, Sylviusweg 72, 2333 BE Leiden, Netherlands

[2]Add2X Biosciences BV, Sylviusweg 72, 2333 CB Leiden, Netherlands.

[3]Current address: Sanquin Plasma Products B.V., Plesmanlaan 125, P.O. Box 26, 1066 CX Amsterdam, the Netherlands

[4]Bioscience, Wageningen University and Research, Droevendaalsesteeg 1, 6708 PB Wageningen, Netherlands

[5] Molecular Biology, Wageningen University and Research, Droevendaalsesteeg 1, 6708 PB Wageningen, Netherlands

[6]Current address: Rijk Zwaan Netherlands B.V., Burgemeester Crezéelaan 40, P.O. Box 40, 2678 ZG De Lier, The Netherlands

Abstract

The ability of plants to undergo embryogenesis is not restricted to fertilized egg cells, as somatic cells can be reprogrammed to totipotent embryonic cells that are able to form differentiated embryos in a process called somatic embryogenesis (SE). SE is induced after treatment with plant hormones, usually the synthetic auxin, 2,4-dichlorophenoxyacetic acid (2,4-D), or through overexpression of certain transcription factor genes. Here we show that the AT-HOOK MOTIF CONTAINING NUCLEAR LOCALIZED 15 (AHL15) protein plays an important role in the acquisition of plant cell totipotency and embryogenesis. *AHL15* overexpression induces formation of somatic embryos on *Arabidopsis thaliana* seedlings in the absence of hormone treatment. By contrast, *ahl15* loss-of-function mutants showed reduced somatic embryo induction in response to 2,4-D treatment or overexpression of the SE-inducing *BABY BOOM* (*BBM*) transcription factor. The *AHL15* gene is bound and transcriptionally-regulated by BBM during SE. During zygotic embryogenesis *AHL15* is expressed in early embryos, where it is required for proper patterning and for development beyond the heart stage. Morphological and cellular analyses showed that a significant number of plants derived from *35S::AHL15* SEs are polyploid. Chromatin staining with fluorescent reporters suggests that AHL15 induces chromatin decondensation which might lead to chromosome missegregation and thus to the occurrence of polyploid cells. Using centromere-specific markers we demonstrated that polyploidisation was caused by endomitotic events that specifically occurred during the initiation of SE. Our findings indicate that *AHL15* is an important driver of plant cell totipotency acquisition, and based on our results, we suggest that opening of the chromatin structure is required for the acquisition of embryonic competency in somatic plant cells.

Keywords: Somatic embryogenesis, AT-HOOK MOTIF CONTAINING NUCLEAR LOCALIZED 15, 2,4-D, BABY BOOM, chromatin decondensation, polyploidy, *Arabidopsis thaliana*

Introduction

The conversion of differentiated somatic cells into embryonic stem cells is a process that occurs in only a few plant species in nature, for example on the leaf margins of *Bryophyllum calycinum* (Yarbrough, 1932) or *Malaxis paludosa* (Taylor, 1967), or from the unfertilized egg cell or ovule cells of apomictic plants (Ozias-Akins and van Dijk, 2007; Hand and Koltunow, 2014). By contrast, for many more plant species, differentiated cells can be converted into embryonic cells under specific laboratory conditions (Birnbaum and Alvarado, 2008; Smertenko and Bozhkov, 2014). The process of inducing embryonic cell fate in differentiated somatic plant tissues is referred to as somatic embryogenesis (SE). Apart from being a tool to study and understand early embryo development, SE is also an important tool in plant biotechnology, where it is used for asexual propagation of (hybrid) crops or for the regeneration of genetically modified plants during transformation (Bhojwani, 2012).

SE is usually induced in *in vitro* cultured tissues by exogenous application of plant growth regulators. The synthetic analog of the plant hormone auxin 2,4-dichlorophenoxyacetic acid (2,4-D) is the most commonly used plant growth regulator for the induction of SE (Gaj, 2001; Jiménez, 2005). During the past two decades, several genes have been identified that can induce SE on cultured immature zygotic embryos or seedlings when overexpressed in the model plant *Arabidopsis thaliana* (Radoeva and Weijers, 2014; Smertenko and Bozhkov, 2014). Several of these genes, including *BABY BOOM* (*BBM*), *WUSCHEL*, and *LEAFY COTYLEDON 1* (*LEC1*) and *LEC2*, have now been recognized as key regulators of SE (Lotan et al., 1998; Stone et al., 2001; Boutilier et al., 2002; Zuo et al., 2002). Recent studies have shown that *LEC2*-induced SE is accompanied by activation of *YUCCA* genes that mediate auxin biosynthesis (Wójcikowska et al., 2013; Stone et al., 2008). However, the molecular mechanisms and key genetic factors that result in the somatic- to embryonic cell fate conversion are still largely unknown.

Here we show that overexpression of *Arabidopsis AT-HOOK MOTIF CONTAINING NUCLEAR LOCALIZED 15* (*AHL15*) can also induce somatic embryos (SEs) on germinating seedlings in the absence of plant growth regulators. AT-hook motifs exist in a wide range of eukaryotic nuclear proteins, and are known to bind to the narrow minor groove of DNA at short AT-rich stretches (Aravind and Landsman, 1998; Reeves, 2010). In mammals, AT-hook motif proteins are chromatin remodelling factors that participate in a wide array of cellular processes, including DNA replication and repair, and gene transcription leading to cell growth, -differentiation, -transformation, -proliferation, and -death (Sgarra et al., 2010). The *Arabidopsis* genome encodes 29 AHL proteins that contain one or two AT-hook motifs and a PPC domain that promotes/directs nuclear localization (Fujimoto et al., 2004; Zhao et al., 2013). *AHL* gene families are found in angiosperms and also in early diverging land plants such as *Physcomitrella patens* and *Selaginella moellendorffii* (Gallavotti et al., 2011; Zhao et al., 2014). *Arabidopsis* AHL proteins have roles in several aspects of plant growth and development, including flowering time, hypocotyl growth (Street et al., 2008; Xiao et al., 2009), flower development (Ng et al., 2009), vascular tissue differentiation (Zhou et al., 2013), and gibberellin biosynthesis (Matsushita et al., 2007). How plant AHL proteins regulate these underlying biological events is largely unknown. Here we show that *AHL15*

and its close homologs (*AHL19*, *AHL20* and *AHL29*) play major roles in directing plant cell totipotency during both zygotic embryogenesis and 2,4-D and BBM-mediated SE. Furthermore, our data show that AHL15 has a role in opening of chromatin, leading to endomitosis and polyploidy in embryonic cells and that *AHL15* overexpression can lead to polyploid SEs and plants, probable by endomitotic events caused by incomplete chromatin condensation during cell division.

Results

AHL genes are sufficient and required for SE induction

To characterize the function of *AHL15*, we generated *Arabidopsis* lines overexpressing *AHL15* under control of the *35S* promoter (*35S::AHL15*). Overexpression seedlings initially remained small and pale and developed very slowly (Fig. S1A,B). Three to four weeks after germination, seedlings from the majority of the transgenic lines (41 of 50 lines) recovered from this growth retardation (Fig. S1C) and continued a relatively normal development, producing rosettes, flowers and finally seeds. However, one- to two weeks after germination, globular structures could be observed on cotyledons of the remaining *35S::AHL15* lines (9 of 50 lines) (Fig. 1A). These structures developed into heart- or torpedo-shaped SEs (Fig. 1B) that could be germinated to produce fertile plants.

In *Arabidopsis*, the cotyledons of immature zygotic embryos (IZEs) are the most competent tissues for SE in response to the synthetic auxin 2,4-D (Gaj, 2001). Remarkably, IZEs from almost all *35S::AHL15* lines were able to produce somatic embryos when cultured on medium lacking 2,4-D. When left on this medium for a longer time, these primary *35S::AHL15* SEs produced secondary SEs (Fig. S2A, B), and in about 20% of *35S::AHL15* lines, this repetitive induction of SEs resulted in the formation of embryonic masses (Fig. S1C). Overexpression of several *Arabidopsis AHL* genes encoding proteins with a single AT-hook motif (the close homologs *AHL19*, *AHL20* and *AHL29* (Fig. S3)), did not induce SEs on germinating seedlings, but did induce SE on low percentage of IZEs in the absence of 2,4-D (not shown). These results suggest that the single AT-hook motif AHL proteins can enhance the embryonic competence of plant tissues, with AHL15 being able to induce a totipotent state already without extra addition of 2,4-D,, the others less so.

Next we investigated the contribution of *AHL* genes to 2,4-D-induced SE, by culturing IZEs from *ahl* loss-of-function mutants on medium containing 2,4-D. Only a slight reduction in SE induction efficiency was observed in the single *ahl15* loss-of-function mutant (Fig. 1C), which stimulated us to examine the contribution of other *AHL* genes in this process. qRT-PCR analysis showed that *AHL15*, *AHL19* and *AHL20* expression was significantly upregulated in IZEs following seven days of 2,4-D treatment (Fig. 1F). Moreover, GUS staining of *AHL15*::*AHL15-GUS* IZEs showed that *AHL15* expression was specifically enhanced in the cotyledon regions where somatic embryos were initiated (Fig. 1D,E). When assessing SE induction, IZEs from double *ahl15 ahl19* loss-of-function mutants carrying an artificial microRNA targeting *AHL20* (*amiRAHL20*; *ahl15 ahl19 amiRAHL20*) produced significantly less SEs (Fig. 1C) and also led to a relative increase in the number of abnormal

SEs or "hairy callus" (Fig.1G). These results indicated that *AHL15* and several homologs are required for 2,4-D-induced somatic embryo formation starting from IZEs.

We noticed that *AHL15::AHL15-GUS* IZEs showed a slightly decreased capacity to form somatic embryos in the presence of 2,4-D (Fig. 1C). Crossing of the *AHL15::AHL15-GUS* reporter into the *ahl15* mutant background induced a strong decrease in the embryogenic capacity of the *ahl15/+ AHL15::AHL15-GUS* IZEs (Fig. 1C). The majority of the IZEs were converted into non-embryogenic calli that were not observed in the other genotypes (Fig. 1G). These results suggest that the chimeric AHL15-GUS protein is inactive and has a dominant negative effect on the other, redundantly acting AHL proteins. This effect is stronger in the *ahl15* loss-of-function mutant, which is in line with the report that AHL proteins form hetero-multimeric complexes with their homologous proteins (Zhao et al., 2013).

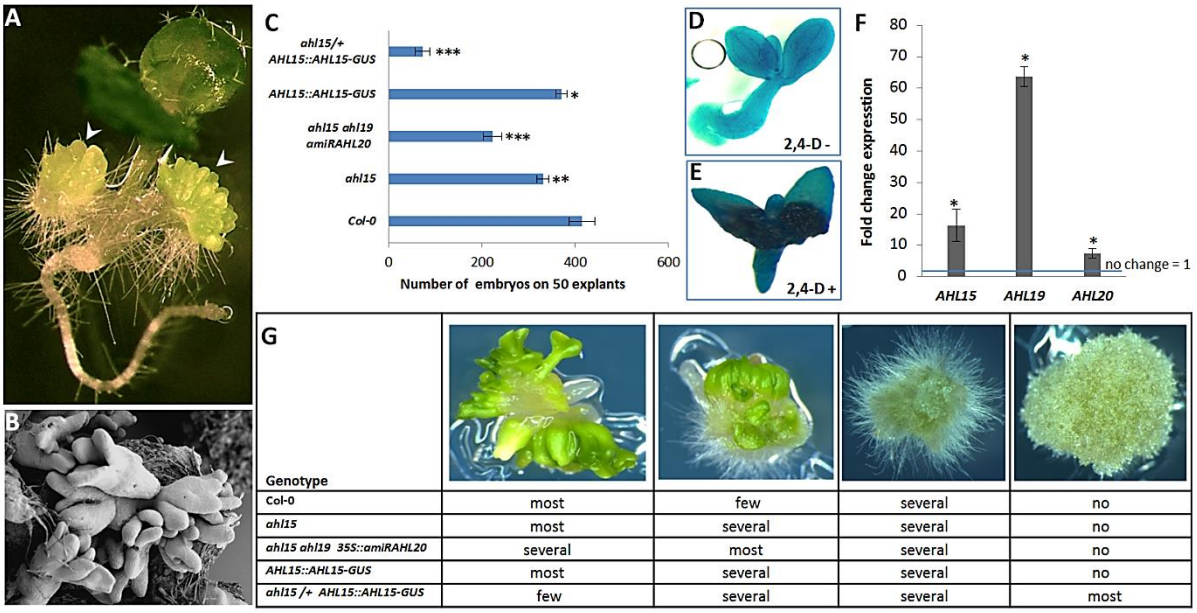

Figure 1 *AHL15* and close homologs are required for SE in *Arabidopsis*. (A) Two-week-old *35S::AHL15 Arabidopsis* seedling with somatic embryossomatic embryos on the cotyledons (arrowheads). (B) Scanning electron micrograph showing torpedo stage somatic embryossomatic embryos on *35S::AHL15* cotyledons. (C) Effects of *ahl* loss-of-function mutations or the presence of the dominant negative *AHL15::AHL15-GUS* fusion construct on the capacity to induce somatic embryossomatic embryos on IZEs by 2,4–D. Asterisks indicate statistically significant differences between the wild type and *ahl* mutant lines, as determined by the Student's *t*-test (* $p<0.05$, ** $p<0.01$, *** $p<0.001$). Error bars indicate standard error of the mean of three biological replicates, with 50 IZEs per replicate. (D, E) Expression of *AHL15::AHL15-GUS* in IZEs cultured for 8 days in the absence (D) or presence (E) of 5 µM 2,4-D. (F) qRT-PCR analysis of *AHL15*, *AHL19*, *AHL20* expression in IZEs cultured for 7 days on medium without and with 5 µM 2,4-D. Asterisks indicate a significant enhancement of *AHL* gene expression in IZEs cultured on medium with 2,4-D compared to medium without 2,4-D (Student's *t*-test, $p < 0.01$). Error bars indicate the standard error of the mean of four biological replicates. (G) Type and proportion of embryo structures and non-embryonic calli on IZEs obtained from wild-type, *ahl15*, *ahl15 ahl19 35S::amiRAHL20*, *AHL15::AHL15-GUS*, and *ahl15/+ AHL15::AHL15-GUS* plants cultured for 2 weeks on 2,4-D medium. The genotype of *ahl15/+ AHL15::AHL15-GUS* calli was verified by PCR analysis.

AHL15 is important during zygotic embryogenesis

Consistent with the critical role of *AHL15* and its close homologs in SE, the involvement of these genes in controlling zygotic embryogenesis was examined. Single and triple *ahl15*, *ahl19* and *ahl20* loss-of-function mutants showed wild-type zygotic embryo (ZE) development. By contrast, siliques of *ahl15/+ AHL15::AHL15-GUS* plants contained brown shrunken seeds (Fig. 2A) that were unable to germinate. The defects could be traced back to abnormal patterns of cell division in globular embryos and arrest at the heart stage in the *ahl15/+ AHL15::AHL15-GUS* ovules (Fig. 2E). We were unable to obtain *ahl15 AHL15::AHL15-GUS* seedlings among 50 F2 plants that we genotyped, suggesting that these patterning defects finally lead to the observed embryo arrest in the homozygous *ahl15 AHL15::AHL15-GUS* embryos. *AHL15::AHL15-GUS* plants produced wild-type embryos (Fig. 2F) and seeds (Fig. 2B), providing additional support for the hypothesis that the dominant negative effect of the AHL15-GUS fusion protein is only observed in the absence of the wild-type AHL15 protein. To confirm that the mutant phenotypes were caused by the dominant negative effect of the chimeric AHL15-GUS fusion protein, an *AHL15::AHL15-GUS* plant line was crossed with an *ahl15 pAHL15::AHL15-TagRFP* line. Unlike *AHL15::AHL15-GUS* lines, *pAHL15::AHL15-tagRFP* lines do not show defects in ZE in *ahl15* background (Fig. 2C). The resulting *ahl15 AHL15::AHL15-GUS AHL15::AHL15-TagRFP* siliques contained WT embryos, indicating that the functional AHL15-TagRFP protein is able to complement the dominant negative effect of the AHL15-GUS fusion (Fig. 2D).

Expression analysis using the *AHL15::AHL15-GUS* and *AHL15::AHL15-tagRFP* lines, both in the wild-type background, showed that *AHL15* is expressed in ZEs from the globular stage onward, with its expression peaking at the bent-cotyledon stage (Fig. 2G-N). In line with the previously reported nuclear localization of AHL proteins (Lim et al., 2007; Ng et al., 2009), the AHL15-TagRFP fusion protein was detected in the nucleus (Fig. 2O).

AHL genes are direct BABY BOOM targets

Overexpression of the AINTEGUMENTA-LIKE (AIL) transcription factor BBM efficiently induces SE in *Arabidopsis* in the absence of exogenous growth regulators (Boutilier et al., 2002). Genome-wide analysis of BBM binding sites using chromatin immunoprecipitation in 2,4-D and *35S::BBM*-induced somatic embryos (ChIP; Horstman et al., 2015) showed that BBM binds to the promoter regions of *AHL15*, *AHL19* and *AHL20* (Fig. 3A-C), suggesting that *AHL* genes are direct downstream BBM targets. To determine whether these genes are also transcriptionally regulated by BBM, we analyzed gene expression changes in *35S::BBM-GR* plants three hours after treatment with dexamethasone (DEX) and the translational inhibitor cycloheximide (CHX). These experiments showed that BBM activated mRNA expression of *AHL15* and *AHL20*, but not yet significantly so for *AHL19* (Fig.3D).

Next, we investigated the requirement for *AHL* genes in *BBM*-induced SE by transforming the *35S::BBM-GR* construct into the triple *ahl15 ahl19 amiRAHL20* and *AHL15::AHL15-GUS* plants. In wild-type Col-0, this construct induced SE in about 7% (40 of 554 transformants) of the primary transformants, which was reduced to 3% in the

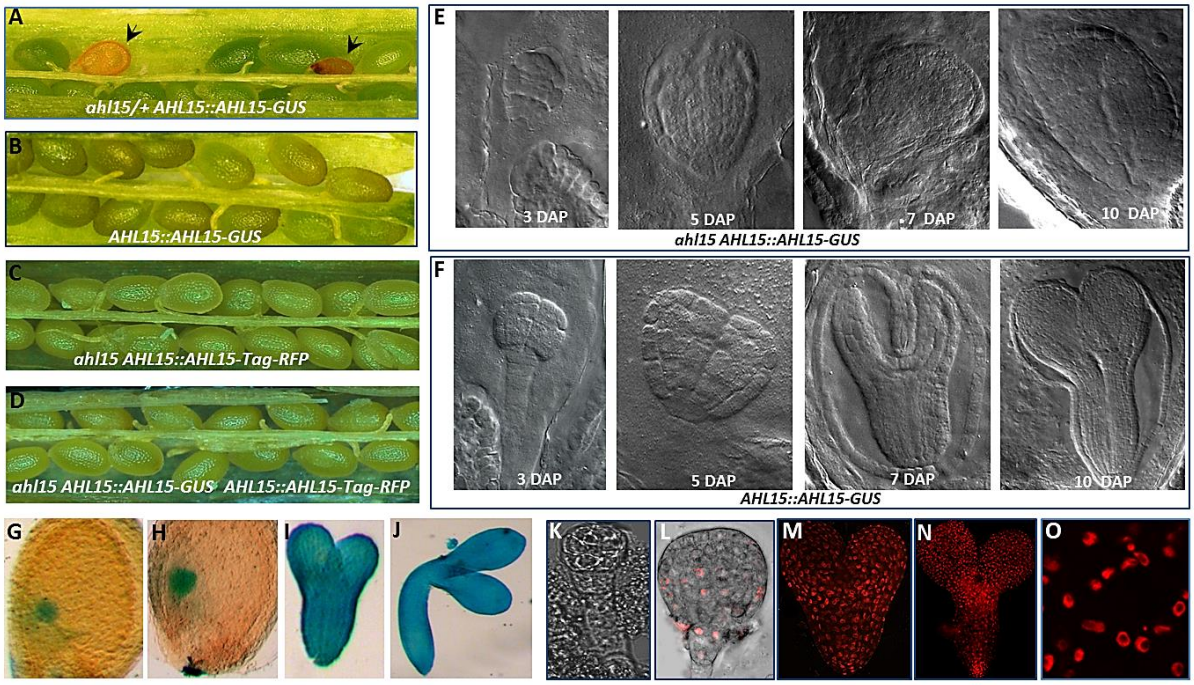

Figure 2 *AHL15* is expressed and essential during ZE. (A) Aberrant development of *ahl15/+ AHL15::AHL15-GUS* seeds (arrowheads). (B-D) Wild-type development of *AHL15::AHL15-GUS* seed (C), *ahl15 AHL15::AHL15-tag-RFP*, (D) and *ahl15 AHL15::AHL15-tag-RFP AHL15::AHL15-GUS* plants. (E,F) DIC images of abnormal zygotic embryo development in siliques of *ahl15/+ AHL15::AHL15-GUS* plants at 3, 5, 7 and 10 days after pollination (DAP, E), and normal zygotic embryo development in siliques of *AHL15::AHL15-GUS* plants at 3, 5, 7 and 10 DAP (F). (G-J) Expression pattern of *AHL15::AHL15-GUS* in globular- (G), heart- (H), torpedo- (I) and bent cotyledon (J) stage embryos. (K-N) Confocal microscopy images of *AHL15::AHL15-tagRFP* early globular- (K), late globular- (L), heart- (M), and torpedo (N) stage embryos. (O) Detail of a torpedo stage embryo showing nuclear localization of AHL15-TagRFP. (K-O) Images show a merge of the transmitted light and the RFP channel (K,L), or the RFP channel alone (M-O)

AHL15::AHL15-GUS background (26 of 801 transformants) and was completely abolished SE in the *ahl15 ahl19 amiRAHL20* background (0 of 351 transformants). These results together with the observation that *AHL15* overexpression, like *BBM* overexpression, induces spontaneous SE suggests that induction of *AHL* gene expression is a key regulatory component of the BBM signaling pathway.

Nuclear *AHL15* modulates the chromatin state in embryonic cells

Based on the observation in animal cells that AT-hook proteins are essential for the open chromatin in neural precursor cells (Catez et al., 2004; Kishi et al., 2012), we investigated whether AHL15 modulates the chromatin structure during SE initiation. Global chromatin structure is characterized by tightly condensed, transcriptionally-repressed regions, called heterochromatin, which can be visualized using fluorescent chromatin markers or DNA staining. Large-scale changes in heterochromatin in somatic plant cells are considered as a sign of cell identity reprogramming (Meister et al., 2011; Bourbousse et al., 2015). Propidium iodide (PI) staining of chromosomal DNA in cotyledon cells of *35S::AHL15* IZEs showed a remarkable disruption of heterochromatin at seven days after culture (Fig. 4A), when

compared to cotyledon cells 3 days after culture (Fig. 4A). In contrast, cotyledon cells of wild-type IZEs did not show a clear change in heterochromatin state between three and seven days (Fig 4A). The *Arabidopsis* HISTONE 2B-GFP protein is incorporated into nucleosomes, providing a marker for the chromatin state in living cells (Bourbousse et al., 2015). H2B-GFP fluorescence observations confirmed that the chromocenters in 7-day-old *35S::AHL15* cotyledon cells (Fig. 4B) were much more diffuse compared to 3-day-old cells (Fig. 4B). No significant differences in H2B-GFP signals were detected between cotyledon cells of three and seven day-incubated wild-type IZEs (Fig 4B). Quantification of the number of detectable chromocenters confirmed that that the number of chromocentres was significantly decreased in cotyledon cells of 7 days incubated *35S::AHL15* IZEs relative to wild-type IZEs (Fig. 4C). This result suggests that AHL15 promotes heterochromatin decondensation. Surprisingly, in cells expressing both *AHL15::AHL15-tagRFP* and *H2B::H2B-GFP* reporters, *AHL15-tagRFP* did not co-localize with the chromocenters (Fig. S4), but showed a more diffuse nuclear distribution, suggesting that the AHL15 regulates global chromatin decondensation.

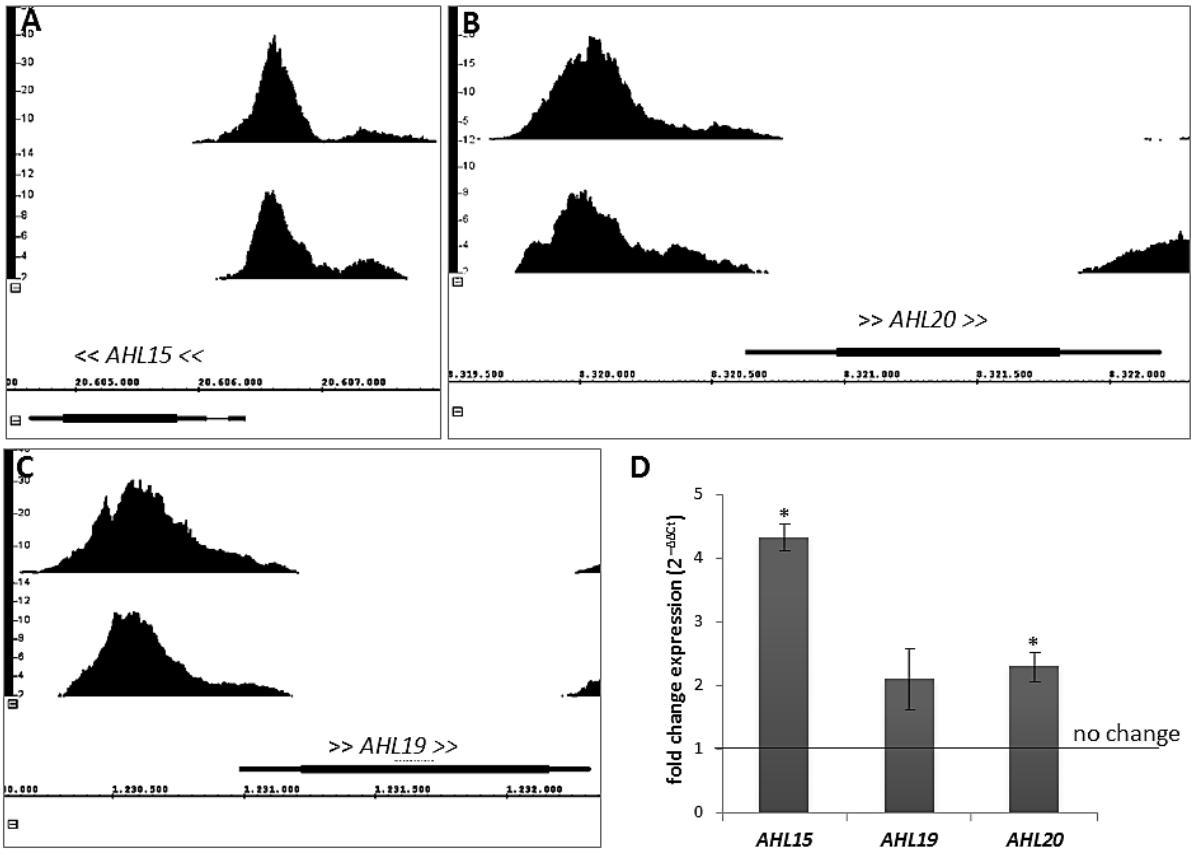

Figure 3 SE-promoting *AHL* genes are direct targets of BBM. (A-C) ChIP-seq BBM binding profiles for *AHL15* (A), *AHL20* (B) and *AHL19* (C). The binding profiles from the *35S::BBM-GFP* (upper profile) and *BBM::BBM-YFP* (lower profile) ChIP-seq experiments are shown. The x-axis shows the nucleotide position of DNA binding in the selected genes (TAIR 10 annotation), the y-axis shows the ChIP-seq score, and the arrow brackets around the gene name indicate the direction of gene transcription. (D) qRT-PCR analysis of the fold change in expression of *AHL* genes in DEX + CHX treated *35S::BBM-GR* seedlings relative to that in DEX + CHX treated Col-0 wild-type seedlings. Asterisks indicate a significant difference in expression levels in *35S::BBM-GR* plants compared to wild-type plants (Student's *t*-test, $p < 0.05$). Error bars indicate standard error of the mean of four biological replicates.

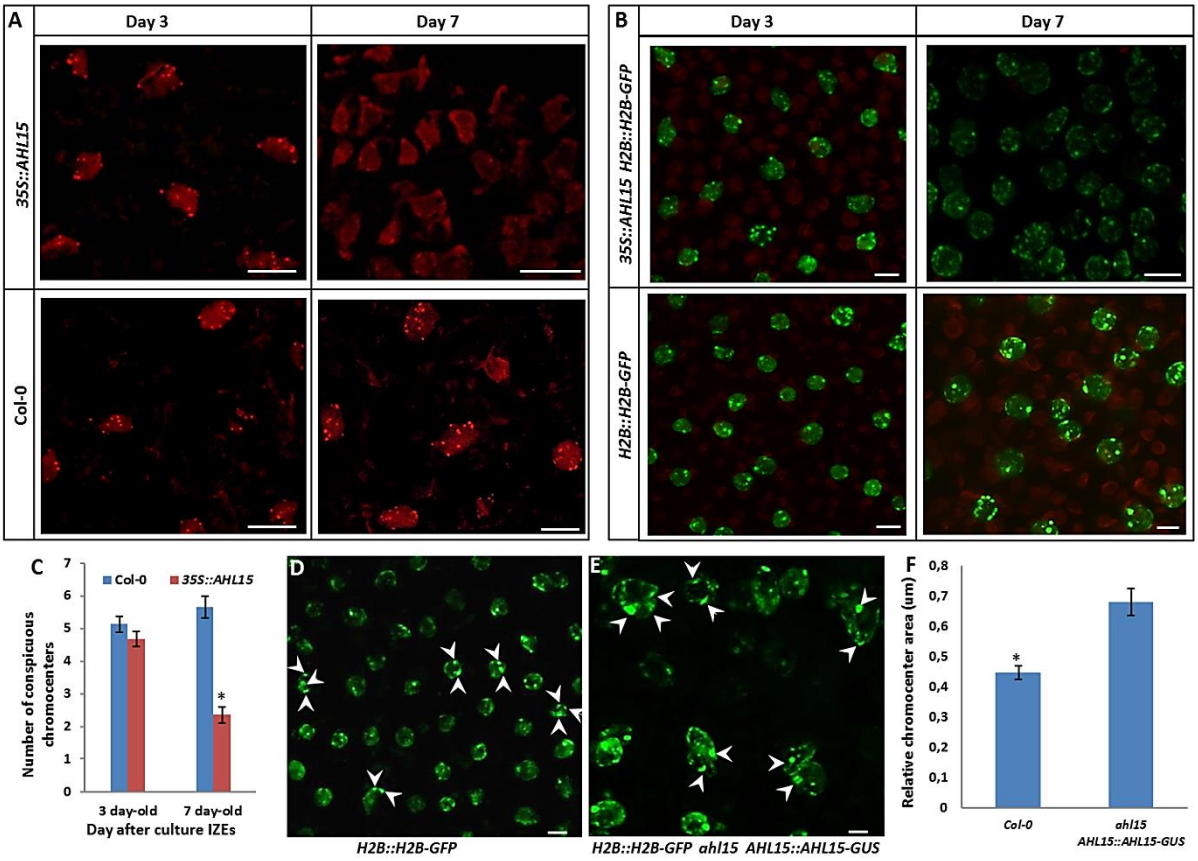

Figure 4 *AHL15* reduces heterochromatin condensation and chromocenter size. (A, B) Visualization of DNA compaction using propidium iodide (PI) staining (A) or H2B-GFP labelling (B) in cotyledon cell nuclei of wild-type and *35S::AHL15* IZEs 3- or 7 days after culture on B5 medium. Size bar indicates 6 µm in A and B. (C) Quantification of the number of conspicuous chromocenters labelled with PI in cotyledon cell nuclei of wild-type and *35S::AHL15* IZEs 3- or 7 days after culture on B5 medium. Error bars indicate standard error of the mean of 4 biological replicates. Statistically significant differences were determined using the Student's *t*-test (* $p<0.01$). (D, E) Visualization of chromocenters using the H2B-GFP reporter in wild-type (D) and defective *ahl15 AHL15::AHL15-GUS* ZEs (E) at 6 DAP. Size bar indicates 3.5 µm in D and E. (F) Quantification of the chromocenter area labelled with H2B-GFP in nuclei of wild-type and *ahl15 AHL15::AHL15-GUS* ZEs at 6 DAP. Error bars indicate standard error of the mean of 6 biological replicates. For each replicate 30 chromocenters were measured (2 or3 of the most clear chromocenters per nucleus), indicated with arrow heads in D and E). Statistically significant differences were determined using the Student's *t*-test (* $p<0.01$).

To obtain insight into the role of AHL15 in chromatin decondensation during zygotic embryogenesis, we introduced the *H2B::H2B-GFP* reporter into the *ahl15/+ AHL15::AHL15-GUS* background. In defective *ahl15 AHL15::AHL15-GUS* embryos, we observed irregular shaped chromocenters that were much larger than those in wild-type cells (Fig. 4D-F). This result together with the reduced heterochromatin condensation observed in cotyledon cells of *35S::AHL15* IZEs suggests that *AHL15* plays a role in regulating the chromatin architecture during embryogenesis.

AHL15 overexpression induces polyploidy during SE initiation

Plants regenerated from somatic embryos obtained from cotyledons of *35S*::*AHL15* IZEs without 2,4-D regularly developed large rosettes with dark green leaves and large flowers (Fig. S5A), phenotypes that were not observed in *35S::AHL15* progeny obtained through ZE. As these phenotypes are typical for polyploid plants, we investigated the ploidy level of the plants. The number of chloroplasts in guard cells (Finn et al., 2011) of plants showing large flowers was two times higher (8-12) than that of diploid wild-type plants (4-6) (Fig. S5B). Moreover, flow cytometry analysis on SE-derived plant lines confirmed that most of these lines were tetraploid, and two were even octoploid (Table 1). The frequency of SE-derived polyploidy varied per *35S::AHL15* line, ranging from 18 to 69% (Table 1). No polyploid plants were obtained from somatic embryos induced by 2,4-D on wild-type IZEs (Table 1), or by *BBM* overexpression (Boutilier et al., 2002) (Table 1), indicating that polyploidisation is specifically induced by *AHL15* overexpression.

Table1. Ploidy level of plants derived from SEs induced by *AHL15* overexpression, *BBM* overexpression or by 2,4-D treatment

Genotype	SE-derived plants	Ploidy level of plants*			ploidy percentage
		2n	4n	8n	
35S::AHL15-2	16	5	11	-	69
35S::AHL15-4	6	4	1	1	33
35S::AHL15-13	11	7	4	-	36
35S::AHL15-14	17	14	2	1	18
35S::AHL15-15	15	11	4	-	27
Col-0, 2,4-D	30	30	-	-	0
35S::BBM	20	20	-	-	0

* The ploidy level was analyzed by counting the chloroplast number in guard cells. For plants derived from *35S::AHL15*-induced SEs, the ploidy level was confirmed using flow cytometry.

Polyploidisation is typically correlated with an increase in cell- and nuclear size in *Arabidopsis* and many other organisms (Tsukaya, 2013). Indeed root cells of tetraploid *35S::AHL15* seedlings showed a larger nucleus and a larger cell volume than diploid control plants (Fig. S5C), explaining the larger organ size observed for these plants. We used the centromere-specific HISTONE3-GFP fusion protein (*CENH3-GFP*) (Fang and Spector, 2005; De Storme et al., 2013) to count the number of chromosomes per cell (Fang and Spector, 2005; De Storme et al., 2013). Seven to eight *CENH3-GFP*-marked centromeric dots could be detected in root cells of wild-type plants and diploid *35S::AHL15* SE-derived plants (Fig S5D). By contrast, around 12-16 centromeric dots were observed in the larger nuclei in root cells of tetraploid *35S::AHL15* plants (Fig S5D). This confirmed that the plants with large organs that were regenerated from *AHL15* overexpression-induced somatic embryos are polyploid.

The considerable frequency polyploid plants were regenerated from *35S::AHL15* somatic embryos posed the question as to when polyploidisation occurs, and whether it is correlated with, or is even promoted by SE induction. We observed a variable number of

CENH3-GFP labelled centromeric dots (6-8, 12-15 and 25-30) per cell in cotyledons of *35S::AHL15* IZEs seven to eight days after of the start of culture, reflecting the presence of diploid, tetraploid and octaploid cells (Fig 5A). No evidence was obtained for polyploidy in root meristems (Fig. S6A) or young leaves (Fig. S6B) of *35S::AHL15* plants propagated through ZE, nor was polyploidy observed in the 2,4-D-induced non-embryogenic calli found on leaf and root tissues of *35S::AHL15* plants (Fig. S6C, D). Based on these results, and in line with the observation that *35S::AHL15* polyploid plants were only obtained from *35S::AHL15* somatic embryos, we conclude that the *AHL15*-induced polyploidisation occurs specifically during in vitro embryogenesis.

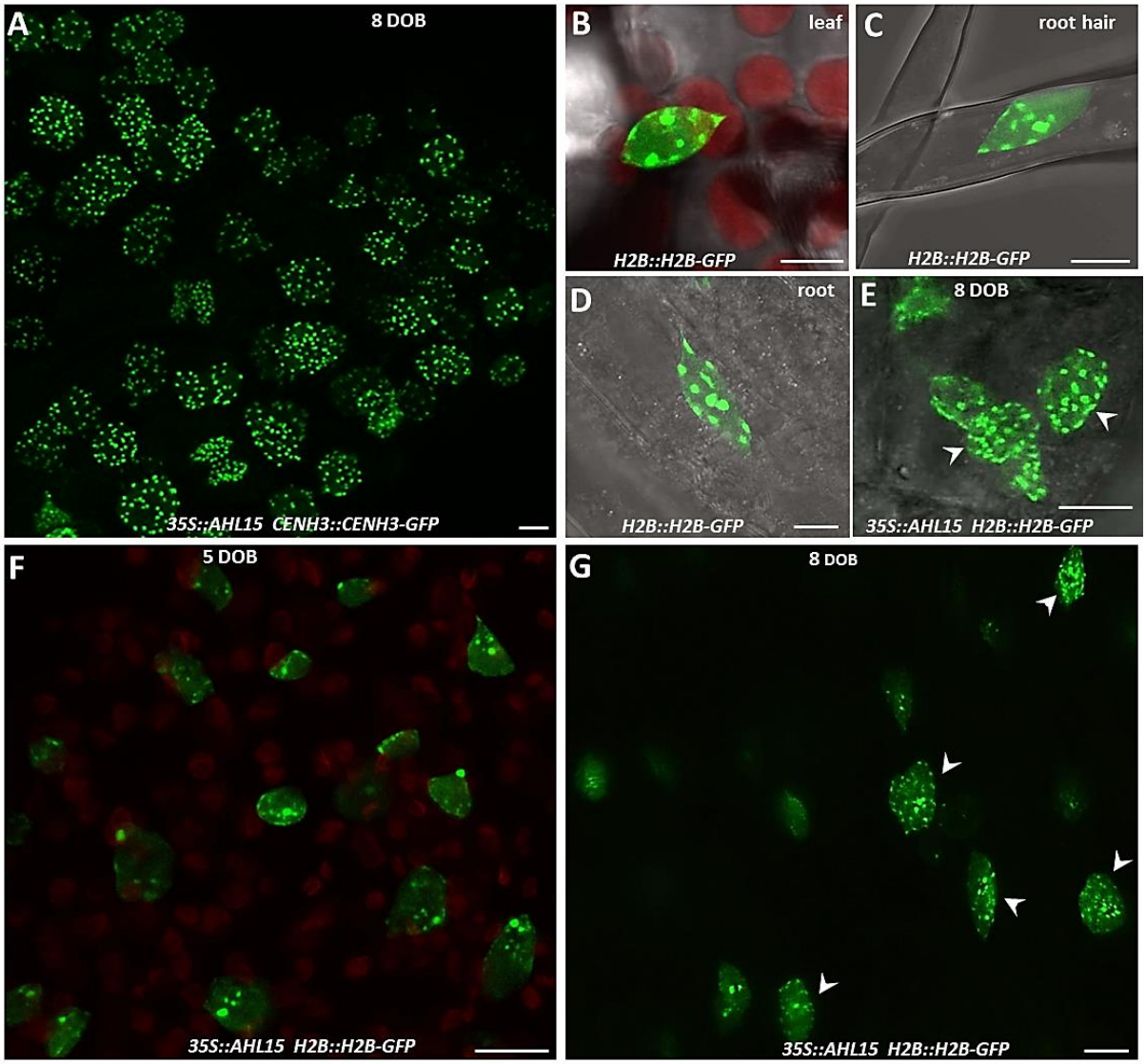

Figure 5 Polyploidy by endomitosis in nuclei of cotyledon cells of cultured *35S::AHL15* IZEs. (A) Confocal image of polyploid cells detected by CENH3-GFP-mediated centromere labeling in an embryonic structure developing on a cotyledon of a *35S::AHL15* IZE cultured for 8 days on B5 medium (DOB). (B-E) Confocal images of H2B-GFP labelled chromocenters in a endoreduplicated nucleus of wild-type cotyledon (B), root hair (C), or root epidermis (D) cell, or in nuclei of cotyledon cells of a *35S::AHL15* IZE cultured for 8 DOB (E). (F, G) H2B-GFP-labelled chromocenters in nuclei of cotyledon cells of *35S::AHL15* IZEs cultured for 5 (F) or 8 (G) DOB. White arrowheads indicate cells with a duplicated number of chromocenters in E and G. Size bars indicate 6 µm. Images show a merge of the transmitted light and the GFP channel (B-E), or the GFP channel alone (A,F,G).

AHL15 overexpression induces endomitosis specifically in somatic embryo progenitor cells

Endoreduplication normally occurs in expanding cells to facilitate cell growth. During endoreduplication duplicated chromosomes do not enter into mitosis and the number of chromocenters does not increase (Edgar and Orr-Weaver, 2001; Lermontova et al., 2006; Lee et al., 2009). We observed an increase in H2B-GFP-marked chromocenters in *35S::AHL15* cotyledon cells that coincided with polyploidisation events (Fig. 5E and G), but not in leaf, root or root hair cells (Fig. 5B-D), suggesting that these polyploid cells are not derived from endoreduplication. Thus duplication of segregated chromosomes in *35S::AHL15* cotyledons cells must be caused by endomitotis, during which mitosis is initiated and chromosomes are separated, but cytokinesis fails to occur. When we followed the H2B-GFP reporter in cotyledons of *35S::AHL15* IZEs, we did not observe any cells with an increased number of chromocenters during the first week of culture, indicating the absence of endomitosis during this period (Fig. 5F). At eight days of IZE culture, however, an increase in chromocenter number could be detected in proliferating *35S::AHL15* cotyledon cells (Fig. 5G). This result showed that cellular polyploidisation in *35S::AHL15* cotyledon cells is tightly associated with the induction of somatic embryos. Although ectopic overexpression of *AHL15* resulted in a high percentage of polyploid plants (Table 1), polyploidy of the embryo itself was no absolute prerequisite for further development of SEs into plants as the most of the *AHL15* expressing plants were still diploid.

Chromosome mis-segregation in *35S::AHL15* cotyledon cells

Disruption of heterochromatin in human mitotic cells leads to mis-segregation of chromosomes (Maison and Almouzni, 2004; Kondo et al., 2008; Carone and Lawrence, 2013; Hahn et al., 2013) and cellular polyploidization (Shi and King, 2005). We hypothesized that heterochromatin disruption and more global chromatin decondensation in dividing *35S::AHL15* cotyledon cells might contribute to endomitosis resulting in polyploid somatic embryo progenitor cells. Compared to normal chromosome segregation (Fig. 6A), chromosome segregation lagged behind (Fig. 6B) and binucleate cells (Fig. 6C-D) could be detected in dividing cotyledon cells of 7-day-old *35S::AHL15* explants. The observation of binucleate cotyledon cells expressing the *WOX2::NLS-YFP* embryo marker (Fig 6E) confirmed that such cells can adopt embryo identity and thus lead to polyploid somatic embryos. Taken together, we conclude that heterochromatin disruption in *35S::AHL15* induced embryonic cotyledon cells may lead to chromosome mis-segregation, the formation of binucleate cells and finally to cellular polyploidization coinciding with the development of polyploid somatic embryos.

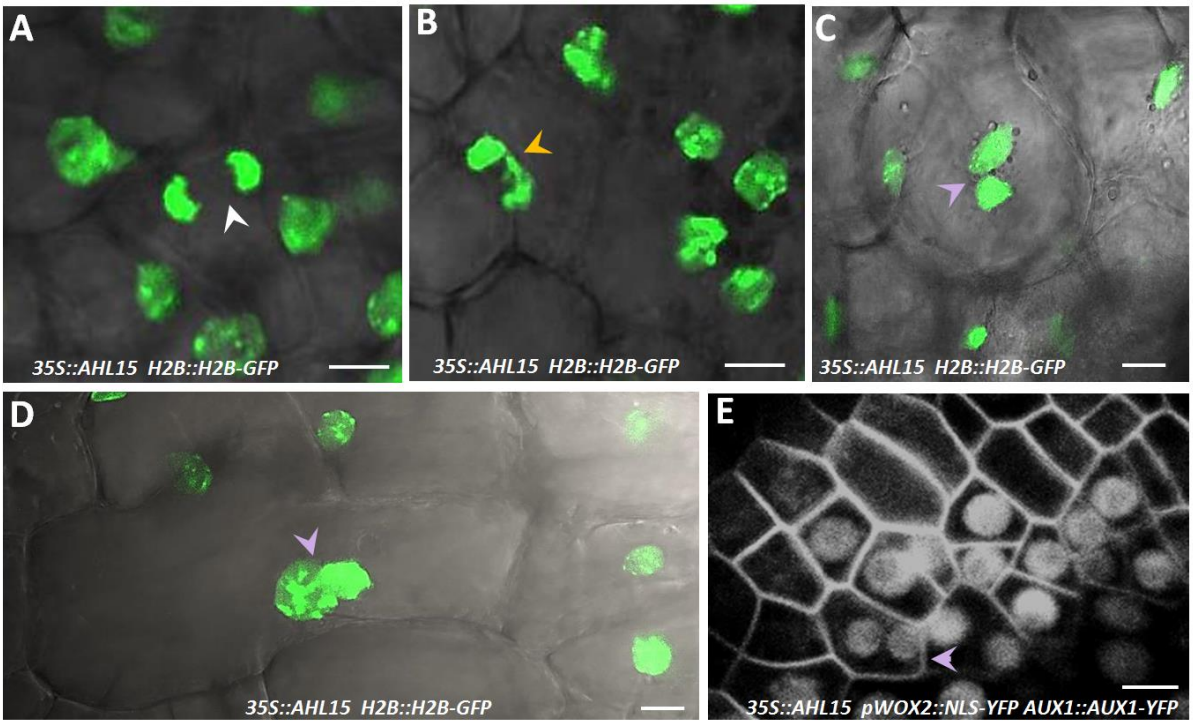

Figure 6 *AHL15* overexpression causes chromosome mis-segregation in IZE cotyledon cells. (A-D) Confocal microscopy analysis of chromosome segregation in cotyledons of *35S::AHL15* IZEs using the H2B-GFP reporter. The white arrowhead indicates normal chromosome segregation during anaphase (A), the yellow arrowhead indicates mis-segregation of chromosomes during anaphase (B), and the magenta arrowhead indicates a bi-nucleated cell (C,D) in cotyledons of *35S::AHL15* IZEs 8 DOB. (E) Confocal microscopy image of a cotyledon of a *35S::AHL15 pWOX2::NLS-YFP pAUX1::AUX1-YFP* IZE. *pWOX2::NLS-YFP* and *pAUX1::AUX1-YFP* reporters were used to mark embryonic nucleus and plasma membranes respectively. The magenta arrowhead indicates a bi-nucleated cell in an area of cells with WOX2-YFP- marked embryo cell fate. Images show a merge of the transmitted light and the GFP channel (A-D), or the YFP channel alone (E). Size bar indicates Size bars indicate 6 µm.

Discussion

The herbicide 2,4-D is extensively used for SE induction in *Arabidopsis* and a wide range of other plant species. In *Arabidopsis*, SE can also be induced on IZEs or seedlings in the absence of 2,4-D treatment by the overexpression of specific transcription factors, such as the AIL transcription factor BBM (Boutilier et al., 2002). In this study, we showed that AHL15 adds to the list of nuclear proteins whose overexpression induces somatic embryos on IZEs and seedlings in the absence of 2,4-D. In line with this observation, AHL15 and its close homologs are upregulated and required for proper SE induction upon 2,4-D treatment. Furthermore, we showed that *AHL15* and its close homologs are downstream targets of BBM, and that they are required for efficient *BBM* overexpression-induced SE.

AT-hook motif-containing proteins are generally considered to be chromatin architecture factors (Catez et al., 2004; Fusco and Fedele, 2007; Sgarra et al., 2010; Kishi et al., 2012). Studies in animals have shown that chromatin decondensation precedes the induction of pluripotent stem cells and their subsequent differentiation (Gaspar-Maia et al., 2011). In the *Arabidopsis* zygote, predominant decondensation of the heterochromatin configuration is

likely to contribute to the totipotency of this cell (Pillot et al., 2010). Our data indicate that *AHL15* overexpression induces a global reduction of the amount of heterochromatin in induced somatic embryonic cells, whereas *ahl* loss-of-function mutants show enhanced heterochromatin formation in *in vitro* cultured explants and also reduces the embryonic competence of these explants. Based on our results, we suggest a model in which chromatin opening is required for the acquisition of embryonic competence in somatic plant cells (Fig. 7). In this model chromatin opening is mediated by upregulation of *AHL* genes, which can be achieved by *35S* promotor-driven overexpression, by 2,4-D treatment or by *BBM* overexpression.

During cell division, eukaryotic cells duplicate their chromosomes after which the mitosis machinery ensures that the sister chromatids segregate equally over the two daughter cells. However, some cell types do not separate the duplicated chromosomes, leading to a polyploidy state known as endopolyploidy (Breuer et al., 2014). In plants, endopolyploidy is commonly classified either endomitosis or endoreduplication (Breuer et al., 2014). In endoreduplication, chromosomes are duplicated during cellular differentiation but do not segregate, leading to the formation of polytene chromosomes (Lermontova et al., 2006). By contrast, during endomitosis sister chromatids are separated, but the last steps of mitosis including nuclear division and cytokinesis are skipped, generally leading to a duplication of the chromosome number. In this work we showed that polyploid cells can be specifically detected during *35S::AHL15* induced SE. The lack of polytene chromosomes suggests that *35S::AHL15*-induced polyploidy is the result of endomitosis.

Previous studies have shown that defects in heterochromatin condensation in animal cells lead to mis-separation of chromosomes during mitosis (Maison and Almouzni, 2004; Kondo et al., 2008; Carone and Lawrence, 2013; Hahn et al., 2013), and that mis-segregation of chromosomes subsequently leads to cellular polyploidisation (Shi and King, 2005). In our experiments, we found a high reduction of heterochromatin coinciding with mis-segregation of chromosomes in in vitro-cultured *35S::AHL15* cotyledon cells. Consistent with the strong conservation of chromosome segregation mechanisms between animal and plant cells (Yanagida, 2005), we propose that cellular polyploidisation in *35S::AHL15* embryonic cells is caused by an AHL15-mediated reduction in chromosome condensation during mitosis, which results in chromosome mis-segregation. The observation that polyploid embryos and plants are not obtained after 2,4-D treatment or by *BBM* overexpression suggests that in these somatic embryos *AHL15* expression levels are not sufficiently elevated to induce a level of chromatin decondensation that leads to chromosome mis-segregation (Fig 7).

A low frequency of polyploid plants derived from somatic embryo culture has been reported (Winkelmann et al., 1998; Borchert et al., 2007; Orbović et al., 2007; Prado et al., 2010), but the molecular and cytological basis for this genetic instability in relation to *in vitro* embryogenesis has not been described. Our data suggest that *AHL15*-mediated polyploidisation could be one factor driving genome duplication events during SE in somatic embryo cultures. AHL15-mediated genome duplication might therefore provide a more efficient means for chromosome doubling of embryos derived from haploid explants such as egg cells or microspores (Soriano et al., 2013) and for the production of polyploid crops.

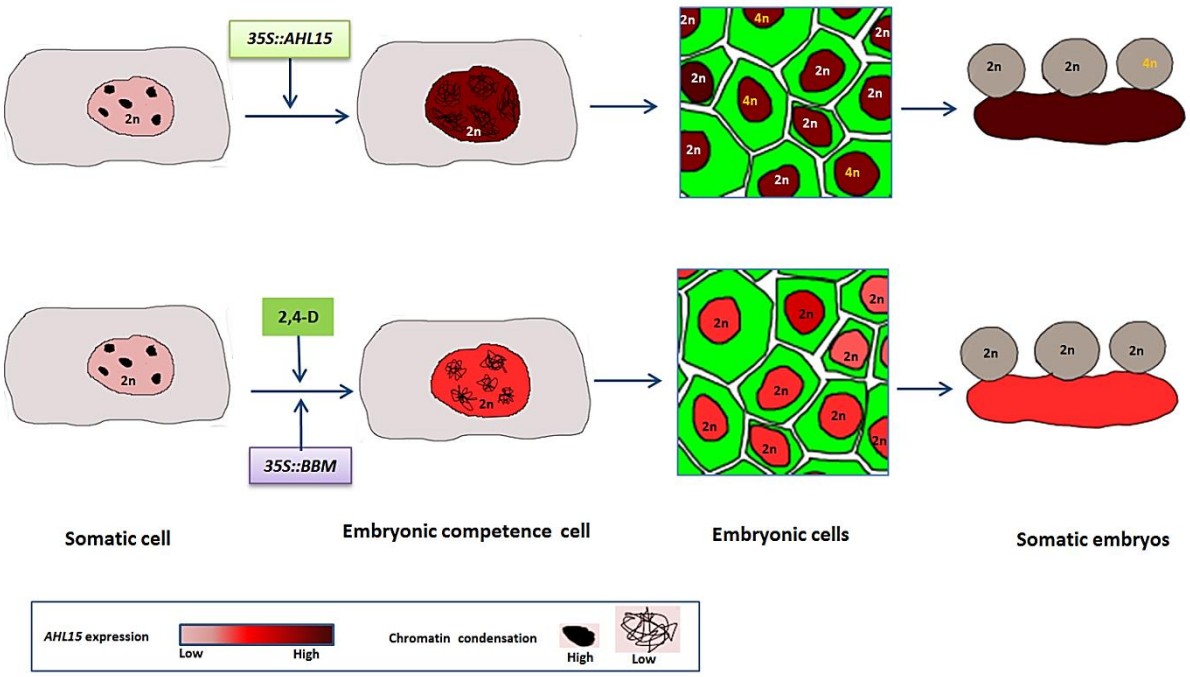

Figure 7 Model for somatic-to-embryonic reprogramming and cellular polyploidization by *AHL15* overexpression. *AHL15* or *BBM* overexpression, or 2,4-D treatment all induce the chromatin decondensation that is required to induce embryonic competence in somatic cells. The high level of chromatin decondensation obtained by *35S* promoter-driven *AHL15* overexpression prevents chromosome segregation in some cells, leading to endomitosis events that give rise to polyploid embryonic cells and subsequently to polyploid somatic embryos. *BBM* overexpression or 2,4-D treatment also lead to enhanced *AHL15* expression resulting in chromatin decondensation sufficient to induce embryonic cells and the resulting somatic embryos, but insufficient to lead to endomitosis, thus only giving rise to diploid somatic embryos.

Methods

Plant material and growth conditions

T-DNA insertion mutants *ahl15* (SALK_040729) and *ahl19* (SALK_070123) were obtained from the European Arabidopsis Stock Centre (http://arabidopsis.info/). Primers used for genotyping are described in Table S1. The reporter lines *CENH3::CENH3-GFP* (Fang and Spector, 2005) and *H2B::H2B-GFP* (Fang and Spector, 2005), *pWOX2::NLS-YFP* (Breuninger et al., 2008), and pAUX1::AUX1-YFP (Swarup et al., 2005) have been described previously. For *in vitro* plant culture, seeds were sterilized in 10 % (v/v) sodium hypochlorite for 12 minutes and then washed four times in sterile water. Sterilized seeds were plated on MA medium (Masson and Paszkowski, 1992) containing 1 % (w/v) sucrose and 0.7 % agar. Seedlings, plants and explants were grown at 21°C, 70% relative humidity, and 16 hours photoperiod.

Plasmid construction and plant transformation

The *35S::AHL15* construct was generated by PCR amplification of the full-length *AHL15* cDNA of (AT3G55560) from ecotype Columbia (Col-0) using primers 35S::AHL15-F and -R (Table S1). The resulting PCR product was cloned as a *Sma*I/*Bgl*II fragment into the *p35S-3'OCS* expression cassette of plasmid pART7, which was subsequently cloned as *Not*I fragment into the binary vector pART27 (Gleave, 1992). To generate the other overexpression constructs, the full-length cDNA clones of *AHL19* (AT3G04570), *AHL20* (AT4G14465), and *AHL29* (AT1G76500) from *Arabidopsis* Col-0 were used to amplify the open reading frames (ORFs) using primers indicated in Table S1. The ORFs were cloned into plasmid pJET1/blunt (GeneJET™ PCR Cloning Kit, #K1221), and next transferred as *Not*I fragments to binary vector *pGPTV 35S::FLAG* (Becker et al., 1992). To generate the *AHL15::AHL15-GUS* and *pAHL15::AHL15-TagRFP* translational fusions, a 4 kb fragment containing the promoter and the full coding region of *AHL15* was amplified using PCR primers AHL15-GUS-F and -R (Table S1), and inserted into pDONR207 using a BP reaction (Gateway, Invitrogen). LR reactions were carried out to fuse the 4 kb fragment upstream of GUS and *tagRFP* in respectively destination vectors pMDC163 (Karimi et al., 2007) and pGD121 (Immink et al., 2012). The artificial microRNA (amiR) targeting *AHL20* was generated as described by Schwab and colleagues (Schwab et al., 2006) using oligonucleotides I-IV miR-a/s AHL20 (Table S1). The fragment of the *amiRAHL20* precursor was amplified using PCR primers amiRNA AHL20-F and –R (Table S1), and subsequently introduced into the entry vector pDONR207 via a BP reaction (Gateway, Invitrogen). The *amiRAHL20* precursor was recombined into destination vectors pMDC32 (Karimi et al., 2007) downstream of the *35S* promoter via an LR reaction (Gateway, Invitrogen). The *p35S::BBM-GR* construct has been described previously (Passarinho et al., 2008). All binary vectors were introduced into *Agrobacterium tumefaciens* strain AGL1 by electroporation (den Dulk-Ras and Hooykaas, 1995) and transgenic *Arabidopsis* Col-0 lines were obtained by the floral dip method (Clough and Bent, 1998).

Somatic embryogenesis

Immature zygotic embryos (IZEs) at the bent cotyledon stage of development (10-12 days after pollination) or germinating dry seeds were used as explants to induce SE using a previously described protocol (Gaj, 2001). In short, seeds and IZEs were cultured on solid B5 medium (Gamborg et al., 1968) supplemented with 5 μM 2,4-D, 2 % (w/v) sucrose and 0.7 % agar (Sigma). Control seeds or IZEs were cultured on solid B5 medium without 2,4-D. To allow further embryo development, explants were transferred to medium without 2,4-D. One week after subculture, the capacity to induce SE was scored under a stereomicroscope as the number of somatic embryos produced from 50 explants cultured on a plate. Three plates were scored for each line. The Student's *t*-test was used for statistical analysis of the data.

Quantitative real-time PCR (qRT-PCR) and ChIP seq analysis

To determine the expression of *AHL* genes during SE induction, RNA was isolated from 25 IZEs cultured for 7 days on B5 medium with or without 2,4-D in 4 biological replicates using a Qiagen RNeasy Plant Mini Kit. The RNA samples were treated with Ambion® TURBO DNA-free™ DNase. To determine the expression of *AHL* genes in 2,4-D treated Col-0 IZEs by qRT-PCR, 1 µg of total RNA was used for cDNA synthesis with the iScript™ cDNA Synthesis Kit (BioRad). PCR was performed using the SYBR-Green PCR Master mix (Biorad) and a CHOROMO 4 Peltier Thermal Cycler (MJ RESEARCH). The Pfaffl method was used to determine relative expression levels (Pfaffl, 2001). Expression was normalized using the *β-TUBULIN*-6 (At5g12250) gene. The gene-specific PCR primers used are described in Table S1.

The effect of *BBM* overexpression on *AHL* gene expression was examined by inducing five-day-old *Arabidopsis thaliana* Col-0 and *35S::BBM-GR* seedlings (four biological replicates for each line) for three hours with 10 µM dexamethasone (DEX) plus 10 µM cycloheximide (CHX). RNA was isolated using the Invitek kit, treated with DNAseI (Invitrogen) and then used for cDNA synthesis with the Taqman cDNA synthesis kit (Applied Biosystems). qRT-PCR was performed as described above. The relative expression level of *AHL* genes was calculated according to the $2^{-\Delta\Delta Ct}$ method (Livak and Schmittgen, 2001), using the wild-type Col-0 value to normalize and the *SAND* gene (At2g28390; (Czechowski et al., 2005) as a reference. The gene-specific PCR primers are listed in Table S1.

The ChIP-seq data and analysis was downloaded from GEO (GSE52400). Briefly, the experiments were performed using somatic embryos from either 2,4-D-induced *BBM::BBM-YFP* cultures (with *BBM::NLS-GFP* as a control) or a *35S::BBM-GFP* overexpression line (with *35S::BBM* as a control), as described in (Horstman et al., 2015).

Ploidy analysis

The ploidy level of plants derived from *35S::AHL15*-induced somatic embryos was determined by flow cytometry (Plant Cytometry Services, Schijndel, Netherlands), and confirmed by counting the total number of chloroplasts in stomatal guard cells and by comparing flower size and or the size of the nucleus in root epidermal cells. The number of chloroplasts in stomatal guard cells was counted for plants derived from 2,4-D- and BBM-induced somatic embryos.

Histological staining and microscopy

Histochemical β-glucuronidase (GUS) staining of *AHL15::AHL15-GUS* IZEs or ovules was performed as described previously (Anandalakshmi et al., 1998) for 4 hours at 37 °C, followed by rehydration in a graded ethanol series (75, 50, and 25 %) for 10 minutes each. GUS stained tissues were observed and photographed using a LEICA MZ12 microscopy (Switzerland) equipped with a LEICA DC500 camera.

DNA staining of wild-type and *35S::AHL15* seedlings was performed using propidium iodide (PI) according to the protocol described by Baroux *et al*. (Baroux et al., 2007). To

stain nuclei, the samples were incubated for 30 minutes in 4′,6-diamidino-2-phenylindole (DAPI) staining solution (1 μg/ml DAPI in phosphate-buffered saline (PBS) just before observation.

For scanning electron microscopy (SEM), seedlings were fixed in 0.1 M sodium cacodylate buffer (pH 7.2) containing 2.5% glutaraldehyde and 2% formaldehyde. After fixation, samples were dehydrated by a successive ethanol series (25, 50, 70, 95, and 100 %), and subsequently critical-point dried in liquid CO_2. Dried specimens were gold-coated and examined using a JEOL SEM-6400 (Japan).

For morphological studies of embryos, fertilized ovules were mounted in a clearing solution (glycerol:water:chloral hydrate = 1:3:8 v/v) and then incubated at 65 °C for 30 min and observed using a LEICA DC500 microscopy (Switzerland) equipped with differential interference contrast (DIC) optics.

The number of chloroplasts in leaf guard cells, the size of the DAPI stained nuclear area in root cells and the number of conspicuous heterochromatin regions of the PI stained nuclei of cotyledon cells were recorded using a confocal laser scanning microscope (ZEISS-003-18533), using a 633 laser, a 488 nm LP excitation and a 650-700 nm BP emission filters for chlorophyll signals in guard cells, a 405 laser, a 350 nm LP excitation and a 425-475 nm BP emission filters for DAPI signals in cotyledon cells, and a 633 laser, 488 nm LP excitation and 600-670 nm emission BP filters for PI signals in cotyledon cells. The relative size chromocenter spots were measured from confocal images by measuring of region of the spots using the measuring region tool of ImageJ software (Rasband).

Cellular and subcellular localization of AHL15-TagRFP and H2B- or CENH3-GFP protein fusions were visualized using the same laser scanning microscope with a 633 laser, and a 532 nm LP excitation and 580-600 nm BP emission filters for TagRFP signals and a 534 laser, 488 nm LP excitation and 500-525 nm BP emission filters for GFP signals.

Acknowledgements

This work is partially supported by Iranian Ministry of Science, Research, and Technology (Grant MSRT 89100156 to O.K.)

References

Anandalakshmi, R., Pruss, G.J., Ge, X., Marathe, R., Mallory, A.C., Smith, T.H., and Vance, V.B. (1998). A viral suppressor of gene silencing in plants. Proc. Natl. Acad. Sci. **95**: 13079-13084.

Aravind, L. and Landsman, D. (1998). AT-hook motifs identified in a wide variety of DNA-binding proteins. Nucleic Acids Res. **26**: 4413–4421.

Baroux, C., Pecinka, A., Fuchs, J., Schubert, I., and Grossniklaus, U. (2007). The triploid endosperm genome of *Arabidopsis* adopts a peculiar, parental-dosage-dependent chromatin organization. Plant Cell **19**: 1782–1794.

Becker, D., Kemper, E., Schell, J and Masterson. A. (1992). New plant binary vectors with selectable markers located proximal to the left T-DNA border. Plant Mol. Biol. **20**: 1195–1197.

Bhojwani, S.S. (2012). Plant tissue culture: applications and limitations (Elsevier B.V.).

Birnbaum, K.D. and Sánchez Alvarado, A. (2008). Slicing across kingdoms: regeneration in plants and animals. Cell **132**: 697–710.

Borchert, T., Fuchs, J., Winkelmann, T., and Hohe, A. (2007). Variable DNA content of Cyclamen persicum regenerated via somatic embryogenesis: rethinking the concept of long-term callus and suspension cultures. Plant Cell. Tissue Organ Cult. **90**: 255–263.

Bourbousse, C., Mestiri, I., Zabulon, G., Bourge, M., Formiggini, F., Koini, M. a, Brown, S.C., Fransz, P., Bowler, C., and Barneche, F. (2015). Light signaling controls nuclear architecture reorganization during seedling establishment. Proc. Natl. Acad. Sci. **112**: E2836–E2844.

Boutilier, K., Offringa, R., Sharma, V.K., Kieft, H., Ouellet, T., Zhang, L., Hattori, J., Liu, C., van Lammeren, A.A.M., Miki, B.L.A., Custers, J.B.M., and van Lookeren, M.M. (2002). Etopic expression of *BABY BOOM* triggers a conversion from vegetative to embryonic growth. Plant Cell **14**: 1737–1749.

Breuer, C., Braidwood, L., and Sugimoto, K. (2014). Endocycling in the path of plant development. Curr. Opin. Plant Biol. **17C**: 78–85.

Breuninger, H., Rikirsch, E., Hermann, M., Ueda, M., and Laux, T. (2008). Differential expression of *WOX* genes mediates apical-basal axis formation in the *Arabidopsis* embryo. Dev. Cell **14**: 867–76.

Carone, D.M. and Lawrence, J.B. (2013). Heterochromatin instability in cancer: from the Barr body to satellites and the nuclear periphery. Semin. Cancer Biol. **23**: 99–108.

Catez, F., Yang, H., Tracey, K.J., Reeves, R., Misteli, T., and Bustin, M. (2004). Network of dynamic interactions between histone h1 and high-mobility-group proteins in chromatin. Mol Cell Biol. **24**:4321-4328.

Clough, S.J. and Bent, F. (1998). Floral dip: a simplified method for *Agrobacterium*-mediated transformation of *Arabidopsis thaliana*. Plant J. **16**: 735–743.

Czechowski, T., Stitt, M., Altmann, T., and Udvardi, M.K. (2005). Genome-wide identification and testing of superior reference genes for transcript normalization in *Arabidopsis* . Plant Physil **139**: 5–17.

Den Dulk-Ras, A. and Hooykaas, P.J.J (1995). Electroporation of *Agrobacterium tumefaciens*. Plant Cell Electroporation Electrofusion Protoc.**55**: 63–72.

Edgar, B. a and Orr-Weaver, T.L. (2001). Endoreduplication cell cycles: more for less. Cell **105**: 297–306.

Fang, Y. and Spector, D.L. (2005). Centromere positioning and dynamics in living *Arabidopsis* plants. Mol Biol Cell. **16**: 5710–5718.

Finn, T.E., Wang, L., Smolilo, D., Smith, N. a, White, R., Chaudhury, A., Dennis, E.S., and Wang, M.-B. (2011). Transgene expression and transgene-induced silencing in diploid and autotetraploid *Arabidopsis*. Genetics **187**: 409–443.

Fujimoto, S., Matsunaga, S., Yonemura, M., Uchiyama, S., Azuma, T., and Fukui, K. (2004). Identification of a novel plant MAR DNA binding protein localized on chromosomal surfaces. Plant Mol. Biol. **56**: 225–239.

Gaj, M.D. (2001). Direct somatic embryogenesis as a rapid and efficient system for in vitro regeneration of *Arabidopsis thaliana*. Plant Cell. Tissue Organ Cult. **64**: 39–46.

Gallavotti, A., Malcomber, S., Gaines, C., Stanfield, S., Whipple, C., Kellogg, E., and Schmidt, R.J. (2011). BARREN STALK FASTIGIATE1 is an AT-hook protein required for the formation of maize ears. Plant Cell **23**: 1756–1771.

Gamborg, O. L., Miller, R., and Ojima, K. (1968). Nutrient requirements of suspension cultures of soybean root cells. Exp. Cell Res. **50**: 151–158.

Gleave, A.P. (1992). A versatile binary vector system with a T-DNA organisational structure conducive to efficient integration of cloned DNA into the plant genome. Plant Mol. Biol. **20**: 1203–1207.

Hahn, M. et al. (2013). Suv4-20h2 mediates chromatin compaction and is important for cohesin recruitment to heterochromatin. Genes Dev. **27**: 859–872.

Hand, M.L. and Koltunow, A.M.G. (2014). The genetic control of apomixis: asexual seed formation. Genetics **197**: 441–450.

Horstman, A., Fukuoka, H., Muino, J.M., Nitsch, L., Guo, C., Passarinho, P., Sanchez-Perez, G., Immink, R., Angenent, G., and Boutilier, K. (2015). AIL and HDG proteins act antagonistically to control cell proliferation. Development **142**: 454–464.

Immink, R.G.H., Posé, D., Ferrario, S., Ott, F., Kaufmann, K., Valentim, F.L., de Folter, S., van der Wal, F., van Dijk, A.D.J., Schmid, M., and Angenent, G.C. (2012). Characterization of SOC1's central role in flowering by the identification of its upstream and downstream regulators. Plant Physiol. **160**: 433–449.

Jiménez, V.M. (2005). Involvement of plant hormones and plant growth regulators on in vitro somatic embryogenesis. Plant Growth Regul. **47**: 91–110.

Karimi, M., Depicker, A., and Hilson, P. (2007). Recombinational cloning with plant gateway vectors. Plant Physiol. **145**: 1144–1154.

Kishi, Y., Fujii, Y., Hirabayashi, Y., and Gotoh, Y. (2012). HMGA regulates the global chromatin state and neurogenic potential in neocortical precursor cells. Nat. Neurosci. **15**: 1127–33.

Kondo, Y., Shen, L., Ahmed, S., Boumber, Y., Sekido, Y., Haddad, B.R., and Issa, J.-P.J. (2008). Downregulation of histone H3 lysine 9 methyltransferase G9a induces centrosome disruption and chromosome instability in cancer cells. PLoS One **3**: e2037.

Lee, H.O., Davidson, J.M., and Duronio, R.J. (2009). Endoreduplication : polyploidy with purpose. Genes Dev.**23**: 2461–2477.

Lermontova, I., Schubert, V., Fuchs, J., Klatte, S., Macas, J., and Schubert, I. (2006). Loading of *Arabidopsis* centromeric histone CENH3 occurs mainly during G2 and requires the presence of the histone fold domain. Plant Cell **18**: 2443–2451.

Lim, P.O., Kim, Y., Breeze, E., Koo, J.C., Woo, H.R., Ryu, J.S., Park, D.H., Beynon, J., Tabrett, A., Buchanan-Wollaston, V., and Nam, H.G. (2007). Overexpression of a chromatin architecture-controlling AT-hook protein extends leaf longevity and increases the post-harvest storage life of plants. Plant J. **52**: 1140–1153.

Livak, K.J. and Schmittgen, T.D. (2001). Analysis of relative gene expression data using real-time quantitative PCR and the 2(-Delta Delta C(T)) Method. Methods **25**: 402–408.

Lotan, T., Ohto, M., Yee, K.M., West, M. a, Lo, R., Kwong, R.W., Yamagishi, K., Fischer, R.L., Goldberg, R.B., and Harada, J.J. (1998). *Arabidopsis LEAFY COTYLEDON1* is sufficient to induce embryo development in vegetative cells. Cell **93**: 1195–1205.

Maison, C. and Almouzni, G. (2004). HP1 and the dynamics of heterochromatin maintenance. Nat. Rev. Mol. Cell Biol. **5**: 296–304.

Masson, Jean and Paszkowski, J. (1992). The culture response of *Arabidopsis thaliana* protoplasts is determined by the growth conditions of donor plants. Plant J. **2**: 829–833.

Matsushita, A., Furumoto, T., Ishida, S., and Takahashi, Y. (2007). AGF1, an AT-hook protein, is necessary for the negative feedback of *AtGA3ox1* encoding *GA 3-oxidas*e. Plant Physiol. **143**: 1152–1162.

Meister, P., Mango, S.E., and Gasser, S.M. (2011). Locking the genome: nuclear organization and cell fate. Curr. Opin. Genet. Dev. **21**: 167–174.

Ng, K.-H., Yu, H., and Ito, T. (2009). AGAMOUS controls *GIANT KILLER*, a multifunctional chromatin modifier in reproductive organ patterning and differentiation. PLoS Biol. **7**: e1000251.

Orbović, V., Ćalović, M., Viloria, Z., Nielsen, B., Gmitter, F.G., Castle, W.S., and Grosser, J.W. (2007). Analysis of genetic variability in various tissue culture-derived lemon plant populations using RAPD and flow cytometry. Euphytica **161**: 329–335.

Ozias-Akins, P. and van Dijk, P.J. (2007). Mendelian genetics of apomixis in plants. Annu. Rev. Genet. **41**: 509–537.

Passarinho, P., Ketelaar, T., Xing, M., van Arkel, J., Maliepaard, C., Hendriks, M.W., Joosen, R., Lammers, M., Herdies, L., den Boer, B., van der Geest, L., and Boutilier, K. (2008). BABY BOOM target genes provide diverse entry points into cell proliferation and cell growth pathways. Plant Mol. Biol. **68**: 225–237.

Pfaffl, M.W. (2001). A new mathematical model for relative quantification in real-time RT-PCR. Nucleic Acids Res. **29**: e45.

Pillot, M., Baroux, C., Vazquez, M.A., Autran, D., Leblanc, O., Vielle-Calzada, J.P., Grossniklaus, U., and Grimanelli, D. (2010). Embryo and endosperm inherit distinct chromatin and transcriptional states from the female gametes in *Arabidopsis*. Plant Cell **22**: 307–320.

Prado, M.J., Rodriguez, E., Rey, L., González, M.V., Santos, C., and Rey, M. (2010). Detection of somaclonal variants in somatic embryogenesis-regenerated plants of Vitis vinifera by flow cytometry and microsatellite markers. Plant Cell, Tissue Organ Cult. **103**: 49–59.

Radoeva, T. and Weijers, D. (2014). A roadmap to embryo identity in plants. Trends Plant Sci: **19**, 709–716.

Reeves, R. (2010). Nuclear functions of the HMG proteins. Biochim. Biophys. Acta - Gene Regul. Mech. **1799**: 3–14.

Schwab, R., Ossowski, S., Riester, M., Warthmann, N., and Weigel, D. (2006). Highly specific gene silencing by artificial microRNAs in *Arabidopsis*. Plant Cell **18**: 1121–1133.

Sgarra, R., Zammitti, S., Lo Sardo, A., Maurizio, E., Arnoldo, L., Pegoraro, S., Giancotti, V., and Manfioletti, G. (2010). HMGA molecular network: From transcriptional regulation to chromatin remodeling. Biochim. Biophys. Acta **1799**: 37–47.

Shi, Q. and King, R.W. (2005). Chromosome nondisjunction yields tetraploid rather than aneuploid cells in human cell lines. Nature **437**: 1038–1042.

Smertenko, A. and Bozhkov, P. V (2014). Somatic embryogenesis: life and death processes during apical-basal patterning. J. Exp. Bot. **65**: 1343–1360.

Soriano, M., Li, H., and Boutilier, K. (2013). Microspore embryogenesis : establishment of embryo identity and pattern in culture. Plant Reprod. **26**: 181–196.

Stone, S.L., Braybrook, S. A, Paula, S.L., Kwong, L.W., Meuser, J., Pelletier, J., Hsieh, T.-F., Fischer, R.L., Goldberg, R.B., and Harada, J.J. (2008). *Arabidopsis LEAFY COTYLEDON2* induces maturation traits and auxin activity: Implications for somatic embryogenesis. Proc. Natl. Acad. Sci. **105**: 3151–3156.

Stone, S.L., Kwong, L.W., Yee, K.M., Pelletier, J., Lepiniec, L., Fischer, R.L., Goldberg, R.B., and Harada, J.J. (2001). *LEAFY COTYLEDON2* encodes a B3 domain transcription factor that induces embryo development. Proc. Natl. Acad. Sci. **98**: 11806–11811.

De Storme, N., De Schrijver, J., Van Criekinge, W., Wewer, V., Dörmann, P., and Geelen, D. (2013). *GLUCAN SYNTHASE-LIKE8* and *STEROL METHYLTRANSFERASE2* are required for ploidy consistency of the sexual reproduction system in *Arabidopsis.* Plant Cell **25**: 387–403.

Street, I.H., Shah, P.K., Smith, A.M., Avery, N., and Neff, M.M. (2008). The AT-hook-containing proteins SOB3/AHL29 and ESC/AHL27 are negative modulators of hypocotyl growth in *Arabidopsis*. Plant J. **54**: 1–14.

Swarup, R., Kramer, E. M., Perry, P., Knox, K., Leyser, H. O., Haseloff, J., and Bennett, M.J. (2005). Root gravitropism requires lateral root cap and epidermal cells for transport and response to a mobile auxin signal. Nat. Cell Biol. **7**: 1057–1065.

Taylor, R.L. (1967). The foliar embryos of *Malaxis paludosa*. Can. J. Bot. **45**: 1553–1556.

Tsukaya, H. (2013). Does ploidy level directly control cell size? Counterevidence from *Arabidopsis* genetics. PLoS One **8**: e83729.

Winkelmann, T., Sangwan, R.S., and Schwenkel, H.-G. (1998). Flow cytometric analyses in embryogenic and non-embryogenic callus lines of *Cyclamen persicum Mill*.: relation between ploidy level and competence for somatic embryogenesis. Plant Cell Rep. **17**: 400–404.

Wójcikowska, B., Jaskóła, K., Gąsiorek, P., Meus, M., Nowak, K., and Gaj, M.D. (2013). *LEAFY COTYLEDON2* (*LEC2*) promotes embryogenic induction in somatic tissues of *Arabidopsis*, via YUCCA-mediated auxin biosynthesis. Planta **238**: 425–440.

Xiao, C., Chen, F., Yu, X., Lin, C., and Fu, Y.-F. (2009). Over-expression of an AT-hook gene, *AHL2*2, delays flowering and inhibits the elongation of the hypocotyl in *Arabidopsis thaliana*. Plant Mol. Biol. **71**: 39–50.

Yanagida, M. (2005). Basic mechanism of eukaryotic chromosome segregation. Phil. Trans. R. Soc. B **360**: 609–621.

Yarbrough, J.A. (1932). Anatomical and developmental studies of the foliar embryos of *Bryophyllum calycinum*. Am. J. Bot. **19**: 443–453.

Zhao, J., Favero, D.S., Peng, H., and Neff, M.M. (2013). *Arabidopsis thaliana* AHL family modulates hypocotyl growth redundantly by interacting with each other via the PPC/DUF296 domain. Proc. Natl. Acad. Sci. **110**: E4688–E4697

Zhao, J., Favero, D.S., Qiu, J., Roalson, E.H., and Neff, M.M. (2014). Insights into the evolution and diversification of the *AT-hook Motif Nuclear Localized* gene family in land plants. BMC Plant Biol. **14**: 2-19

Zhou, J., Wang, X., Lee, J.-Y., and Lee, J.-Y. (2013). Cell-to-cell movement of two interacting AT-hook factors in *Arabidopsis* root vascular tissue patterning. Plant Cell **25**: 187–201.

Zuo, J., Niu, Q.-W., Frugis, G., and Chua, N.-H. (2002). The *WUSCHEL* gene promotes vegetative-to-embryonic transition in *Arabidopsis*. Plant J. **30**: 349–359.

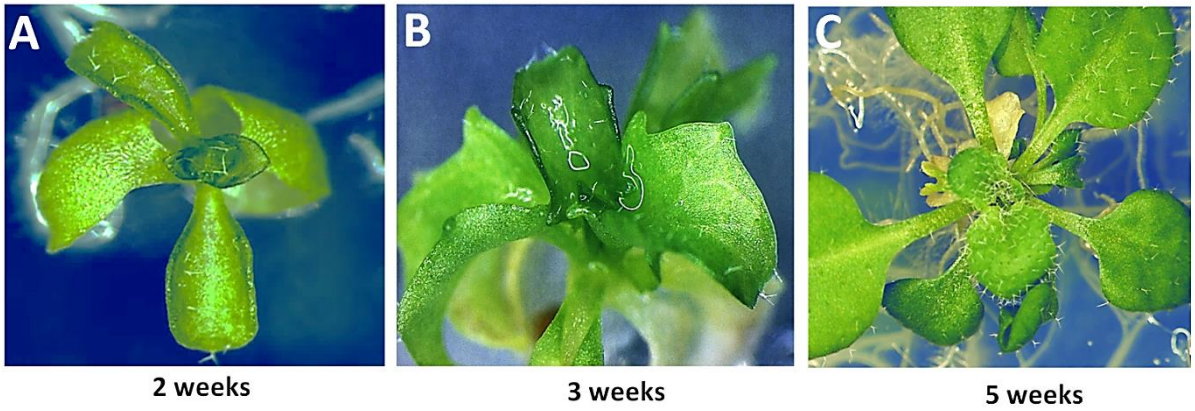

Supplementary figure 1 *AHL15* overexpression represses seedling development in *Arabidopsis*. (A-C) The morphology of 2 (A), 3 (B), and 5 (C)-week-old *35S::AHL15* plants were grown in long day conditions (16 hr light/ 8 hr dark).

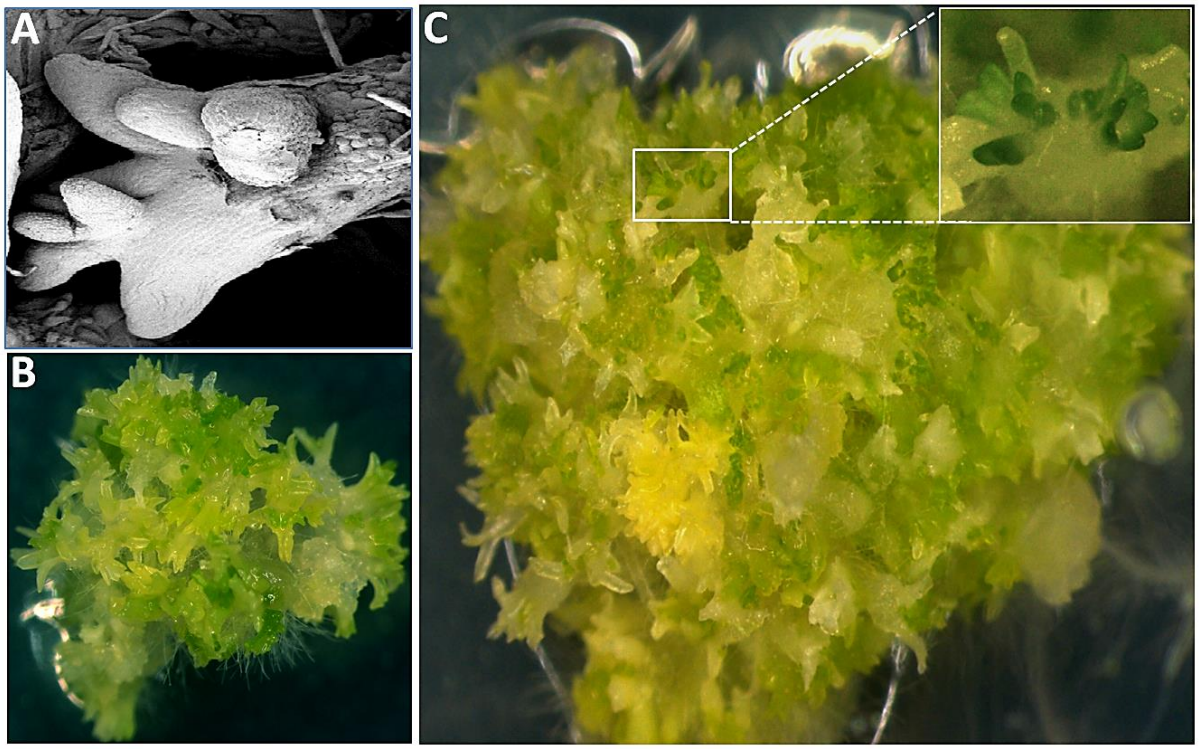

Supplementary figure 2 *AHL15* overexpression induces reiterative somatic embryo initiation resulting in embryonic masses. (A) Scanning electron micrograph showing the secondary somatic embryos formed on a 35S::AHL15 primary somatic embryo. (B) The morphology of a 3-week-old *AHL15*-induced embryonic mass following secondary SE. (C) The morphology of a 2-month-old embryonic mass formed from a *35S::AHL15* seedling.

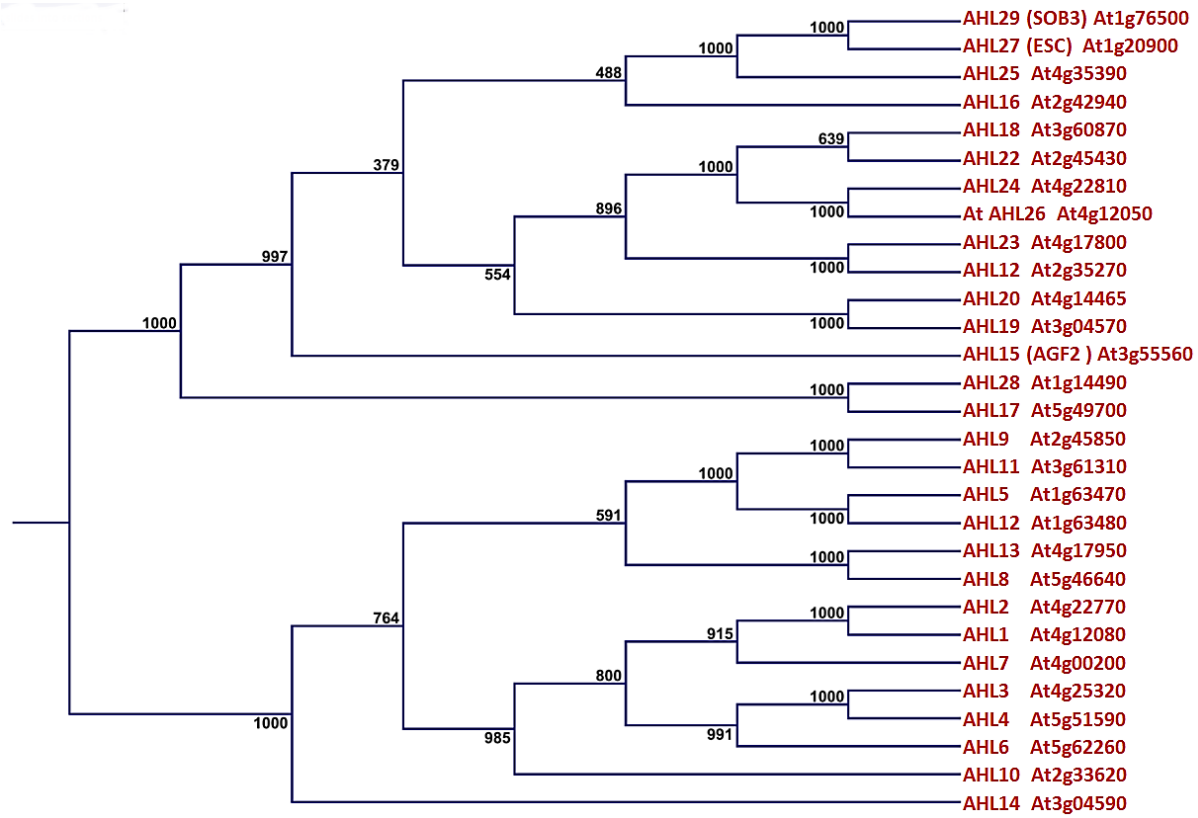

Supplementary figure 3 A phylogenetic tree of the *Arabidopsis AHL* gene family.

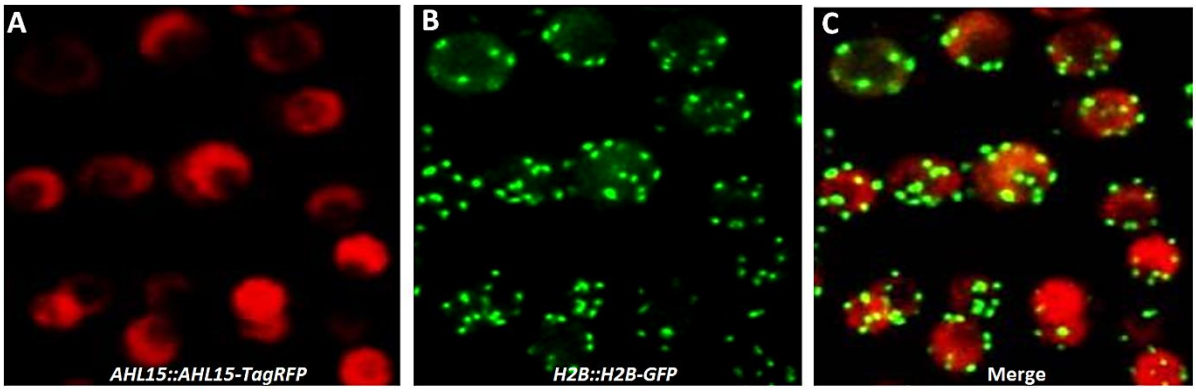

Supplementary figure 4 AHL15-TagRFP does not co-localize with H2B-GFP-marked heterochromatin. (A-C) Confocal images of root meristem cells. The RFP channel showing nuclear-localized AHL15-tagRFP (A), the GFP channel showing H2B-GFP marked heterochromatin (B), and the merged images (C).

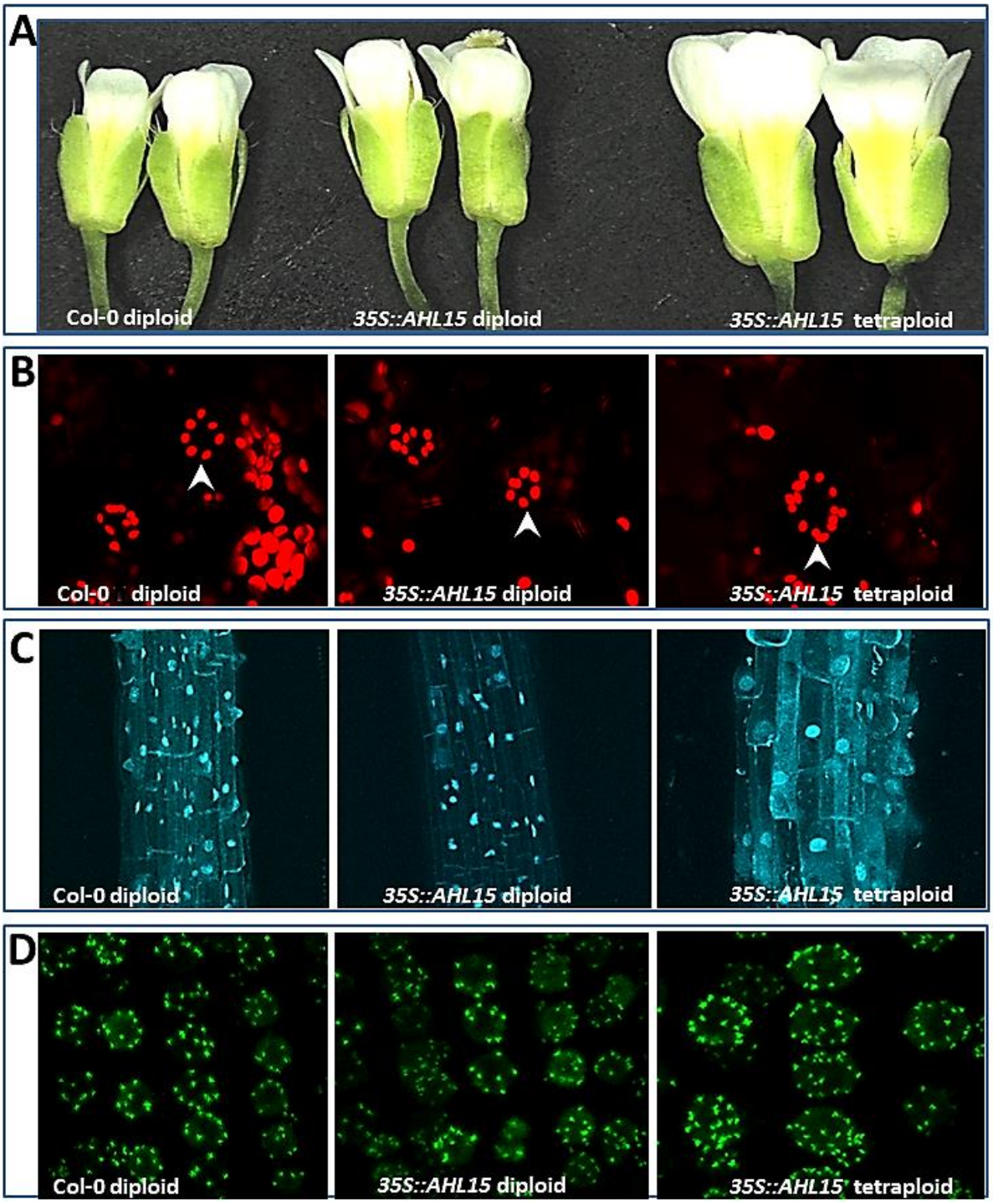

Supplementary figure 5 Plants regenerated from *35S::AHL15*-induced somatic embryos are frequently polyploid. (A-D) Analysis of wild-type *Arabidopsis* (left), and a diploid plant line (middle), and a tetraploid plant line (right) each regenerated from an *35S::AHL15*-induced somatic embryo. (A) Tetraploid *35S::AHL15* plants show increased organ size compared to the diploid control plants, as demonstrated by the size of the flower organs. (B-D) Tetraploid *35S::AHL15* plants have twice the number/a higher number of chloroplasts in guard cells (marked by arrow heads, B), show root cells with a larger nucleus and cell size (C), and show a duplication in the CENH3-GFP-labelled centromeres (D) compared to wild-type and diploid *35S::AHL15 Arabidopsis* plants.

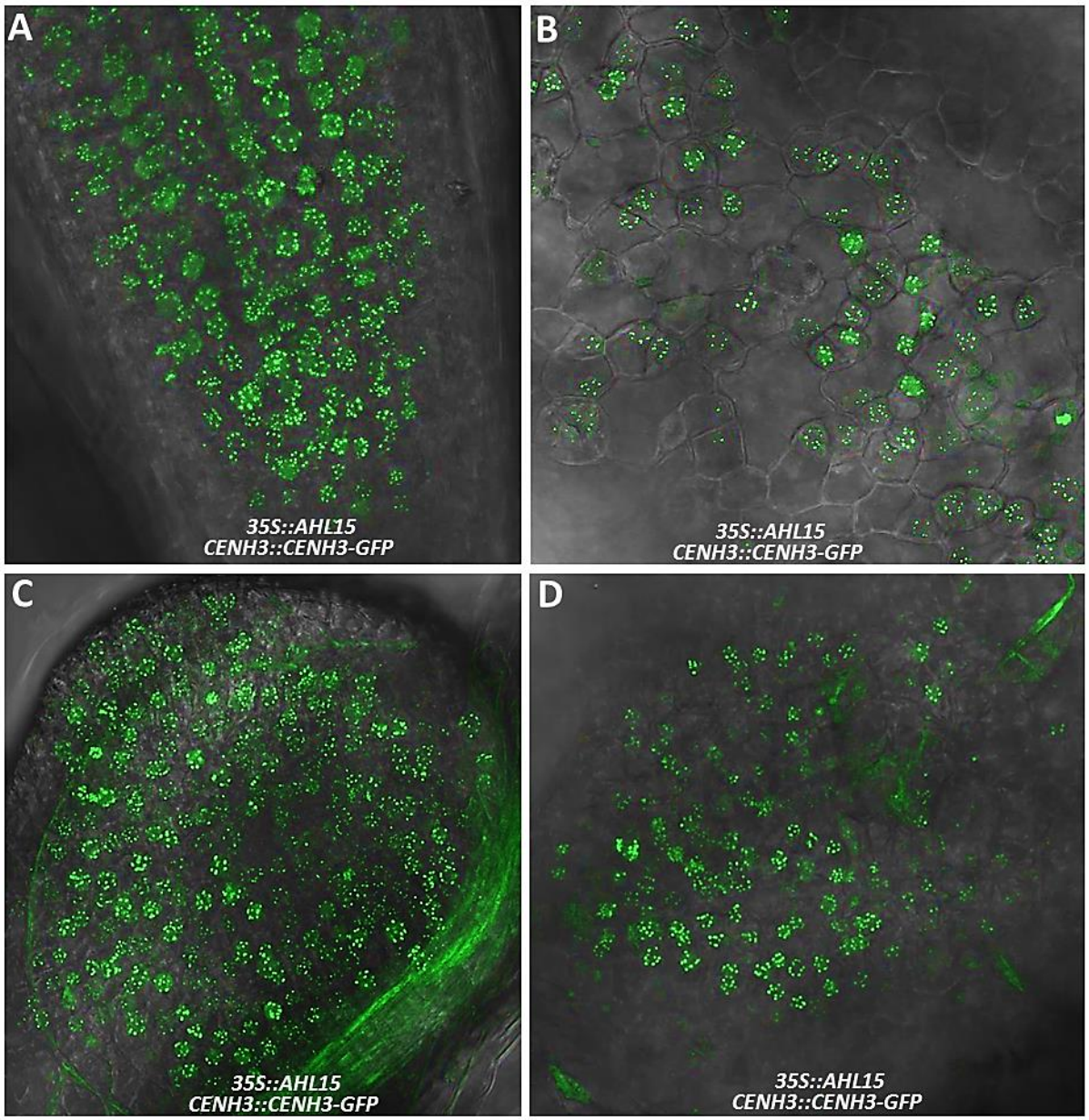

Supplementary figure 6 Endoploidy does not occur in *35S::AHL15* leaves and roots. (A-D) CENH3-GFP–mediated centromere labeling in cells of a root tip (A), a young leaf (B), or in cells of 2,4-D-induced callus on a root (C), or a young leaf (D).

Supplementary Table 1: Primers used for cloning, genotyping and qRT-PCR (F: forward; R: reverse)

Name	Sequence (5' to 3')	Purpose
35S::AHL15-F	CCCGGGATGGCGAATCCTTGGTGGGTAG	*35S::AHL15* construct
35S::AHL15-R	GGATCCTCAATACGAAGGAGGAGCACG	
35S::AHL29-F	ATAAGAATGCGGCCGCGACGGTGGTTACGATCAATC	*35S::AHL29* construct
35S::AHL29-R	ATAGTTTAGCGGCCGCCTAAAAGGCTGGTCTTGGTG	
35S::AHL20 –F	ATAAGAATGCGGCCGCGCAAACCCTTGGTGGACGAAC	*35S::AHL20* construct
35S::AHL20-R	ATAGTTTAGCGGCCGCTCAGTAAGGTGGTCTTGCGT	
35S::AHL19-F	GGGGACAAGTTTGTACAAAAAAGCAGGCTCGATGGCG AATCCATGGTGGAC	*35S::AHL19* construct
35S::AHL19-R	GGGGACCACTTTGTACAAGAAAGCTGGGTAAACAAGT AGCAACTGACTGG	
AHL15-GUS-F	GGGGACAAGTTTGTACAAAAAAGCAGGCTCGACACTCC TCTGTGCCACATT	*AHL15::AHL15-GUS* construct
AHL15-GUS-R	GGGGACCACTTTGTACAAGAAAGCTGGGTAATACGAAG GAGGAGCACGAG	*AHL15::AHL15-tagRFP*
I miR-s AHL20	GATTAGACTACCTCAAATTGCTATCTCTCTTTTGTATTCC	
II miR-a AHL20	GATAGCAATTTGAGGTAGTCTAATCAAAGAGAATCAATGA	
III miR*s AHL20	GATAACAATTTGAGGAAGTCTATTCACAGGTCGTGATATG	*35S::amiRAHL20* construct
IV miR*a AHL20	GAATAGACTTCCTCAAATTGTTATCTACATATATATTCCT	
amiRNA AHL20-F	GGGGACAAGTTTGTACAAAAAAGCAGGCTCGCGACGGT ATCGATAAGCTTG	
amiRNA AHL20-R	GGGGACCACTTTGTACAAGAAAGCTGGGTACCCATGGCG ATGCCTTAAAT	
SALK_040729-F	GTCGGAGAGCCATCAACACCA	ahl15 genotyping
SALK_040729-R	CGACGACCCGTAGACCCGGATC	
SALK_070123-F	GGCGAATCCATGGTGGACAGG	ahl19 genotyping
SALK_070123-R	GGCCGCTCATCTGTCCTCCTC	
qAHL15-F	AAGAGCAGCCGCTTCAACTA	qRT-PCR *AHL15*
qAHL15-R	TGTTGAGCCATTTGATGACC	
qAHL20-F	CAAGGCAGGTTTGAAATCTTATCT	qRT-PCR *AHL120*
qAHL20-R	TAGCGTTAGAGAAAGTAGCAGCAA	
qAHL19-F	CTCTAACGCGACTTACGAGAGATT	qRT-PCR *AHL19*
qAHL19-R	ATATTATACACCGGAAGTCCTTGGT	
qβ-TUBULIN-6-F	TGGGAACTCTGCTCATATCT	qRT-PCR *TUBULIN-6*
qβ-TUBULIN-6-R	GAAAGGAATGAG GTTCACTG	
qSAND-F	AACTCTATGCAGCATTTGATCCACT	qRT-PCR *SAND*
qSAND-R	TGATTGCATATCTTTATCGCCATC	

*, F: forward; R: reverse